Supporting Information (SI)

for

4-Phenoxyphenol-Functionalized Reduced Graphene Oxide Nanosheets: A Metal-Free Fenton-Like Catalyst for Pollutant Destruction

Lai Lyu[abc], *Guangfei Yu*[c], *Lili Zhang*[c], *Chun Hu**[,abc] *and Yong Sun*[d]

[a]School of Environmental Science and Engineering, Guangzhou University, Guangzhou, 510006, China

[b]Research Institute of Environmental Studies at Greater Bay, Guangzhou University, Guangzhou, 510006, China

[c]Key Laboratory of Drinking Water Science and Technology, Research Center for Eco-Environmental Sciences, Chinese Academy of Sciences, Beijing 100085, China

[d]College of Aerospace and Civil Engineering, Harbin Engineering University, Harbin 150001, China

*Corresponding author: Chun Hu Ph.D./Professor, e-mail: huchun@gzhu.edu.cn

Number of pages: 25

Number of figures: 18

Number of tables: 1

Supplementary Experimental Section:

Chemicals and reagents. 4-Phenoxyphenol (POP, ≥98%) was obtained from Aladdin (Shanghai, China). 5-Tert-butoxycarbonyl-5-methyl-1-pyrroline-N-oxide (BMPO, 99%), horseradish peroxidase (POD, 99%), *N*,*N*-diethyl-*p*-phenylenediamine sulfate (DPD, 98%) and 2-chlorophenol (2-CP, ≥99%) were purchased from Sigma-Aldrich (St. Louis, USA). Bisphenol A (BPA, ≥99%) was obtained from Acros (Geel, Belgium). Hydrogen peroxide (H_2O_2, 30%, w/w), graphite powder (99.85%) and all of the other chemicals (analytical grade) were purchased from Sinopharm Chemical Reagent Co. (Shanghai, China). Deionized water was used throughout this study.

Synthesis of GO. Graphene oxide (GO) was prepared by a modified Hummers method through oxidation of graphite powder.[1, 2] Typically, 5.0 g graphite was placed into 115 mL of cold concentrated H_2SO_4 solution in an ice bath below 0 °C. Then, 25.0 g $NaNO_3$ was added to the solution, which was magnetically stirred for 30 min. $KMnO_4$ (15.0 g) was then gradually added to the above mixture under stirring, and the temperature of the mixture was kept below 0 °C for 3.0 h. The mixture was then transferred to a water bath and magnetically stirred at 38 °C for 30 min. After that, 250 mL deionized water was slowly added to the mixture under stirring, and the temperature of the mixture was raised to 95 °C. After reacting for 1.0 h, 50 mL H_2O_2 (30 wt%) was added into the above solution to quench the reaction and produce a golden-brown solution. The sample was subsequently washed with diluted HCl solution and deionized water dozens of times via centrifugation until the pH of the washing solution was ~6. Finally, the product was dried at 70 °C to obtain the solid GO sample.

Characterization. Powder X-ray diffraction (XRD) patterns of all samples were recorded in the range of 5−90°(2θ) on a Scintag-XDS-2000 diffractometer with Cu Kα radiation (λ = 1.540598 Å) operating at 40 kV and 40 mA. The structure and morphology of POP-rGO NSs were observed by high-resolution transmission electron microscopy (HRTEM, JEOL-2010), using an acceleration voltage of 200 kV. IR spectra of the samples, as KBr pellets, were recorded in the range of 4000-400 cm^{-1} using a Nicolet 8700 FTIR spectrophotometer (Thermo Fisher Scientific Inc., USA). Raman spectra were recorded on a LabRAM HR Evolution (HORIBA, France) equipped with a CCD detector using a laser source at an excitation line of 532 nm. X-ray photoelectron spectroscopy (XPS) data were recorded on an AXIS-Ultra instrument using monochromatic Al Kα radiation (225 W, 15 mA, 15 kV) and low-energy electron flooding for charge compensation. The binding energies were calibrated using the C1s hydrocarbon peak at 284.8 eV. Electron paramagnetic resonance (EPR) spectra of the solid samples were obtained using a Bruker model A300-10/12 electron paramagnetic resonance spectrometer. The solid-state ^{13}C direct single pulse magic angle spinning (MAS) nuclear magnetic resonance (NMR) spectra were recorded on a JNM-ECZ600R NMR spectrometer. The samples were packed into a 3.2 mm rotor and spun at 12 kHz using 5 s relaxation delays.

Detection of $^{\bullet}OH$ and $O_2^{\bullet-}$ EPR signals. BMPO-trapped EPR signals were detected in different air-saturated methanol/aqueous dispersions of the corresponding samples using a Bruker A300-10/12 EPR spectrometer at room temperature. Typically, in the absence of H_2O_2, 0.05 g of the prepared powder sample was added to 1 mL of water (for detecting $^{\bullet}OH$) or water/methanol (10:90, *v/v*, for detecting $O_2^{\bullet-}$). Then, 20 μL of BMPO (250 mM) was added, and the solution was allowed to stand for 5 min. The

solution was then sucked into a capillary for detection. In the presence of H_2O_2, 0.01 g of the prepared powder sample was added to 1 mL of water (for detecting $^{\bullet}OH$) or methanol (for detecting $O_2^{\bullet-}$). Then, 90 μL of the above suspension, 5 μL of BMPO (250 mM), and 5 μL of H_2O_2 (30%, *w/w*) were mixed and allowed to stand for 5 min. The solution was than sucked into a capillary tube to carry out EPR detection.

DFT calculations. The models of different graphene fragments with an O atom located in different positions were created using GaussView 5.0. The dangling bonds of the edge atoms were terminated with H atoms to obtain a neutral cluster. All calculations were performed with the Gaussian 09 program. The B3LYP/6-31g(d) method was used to optimize the models. The ESP distributions were constructed with GaussView 5.0 on the basis of the B3LYP/6-31g(d)-optimized results. Due to the size and edge effects, the properties estimated with the finite-size model may vary from those of the real system to some extent. However, it can be expected that the results obtained with the current model would be qualitatively reliable in predicting the local chemical properties.

Supplementary Figures:

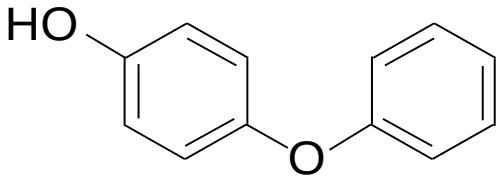

4-phenoxyphenol (POP)

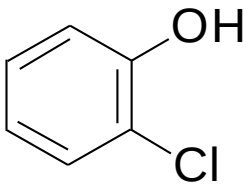

2-chlorophenol (2-CP)

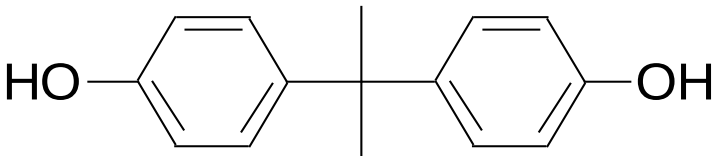

bisphenol A (BPA)

Figure S1. Structure of 4-phenoxyphenol (POP, *p*-hydroxydiphenyl ether), 2-chlorophenol (2-CP) and bisphenol A (BPA).

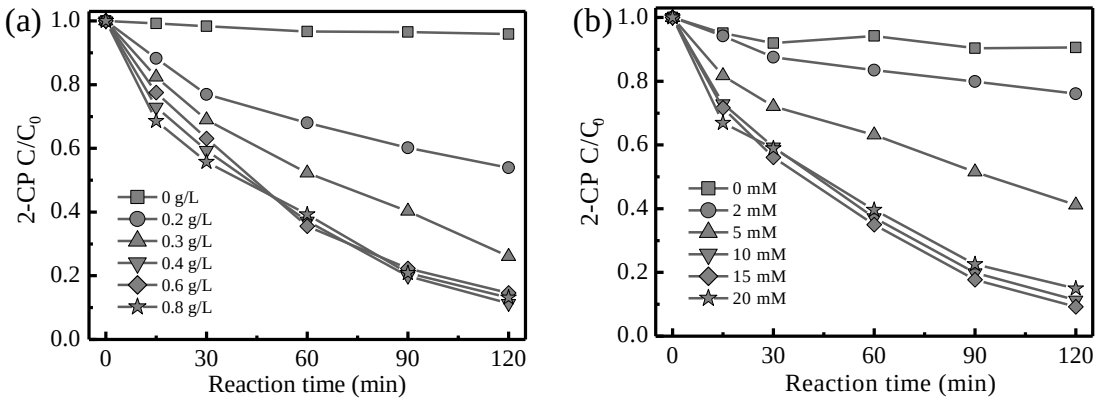

Figure S2. Effect of (a) catalyst concentration and (b) H_2O_2 dosage on 2-CP degradation in the POP-rGO NSs suspension. Reaction conditions: initial pH 6.5, initial 2-CP 10 ppm, initial H_2O_2 10 mM (for a), catalyst 0.4 g L^{-1} (for b).

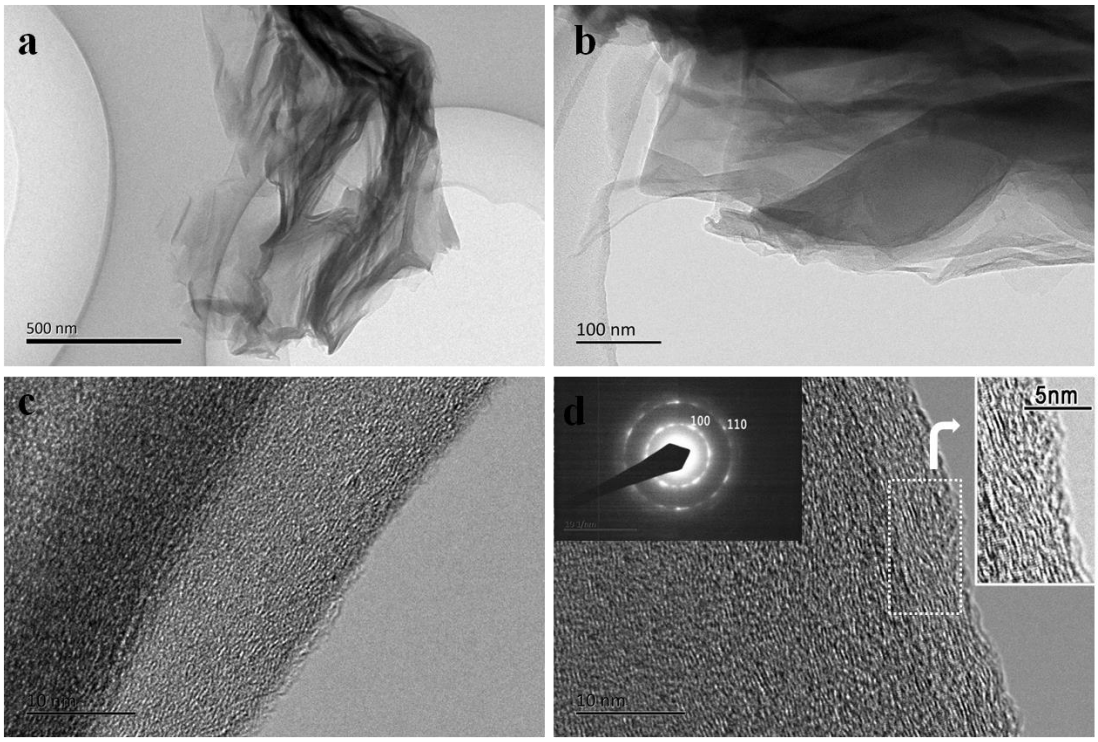

Figure S3. TEM images of POP-rGO NSs. (a) and (b) low magnifications. (c) and (d) high magnifications. The inset is the resultant SAED pattern.

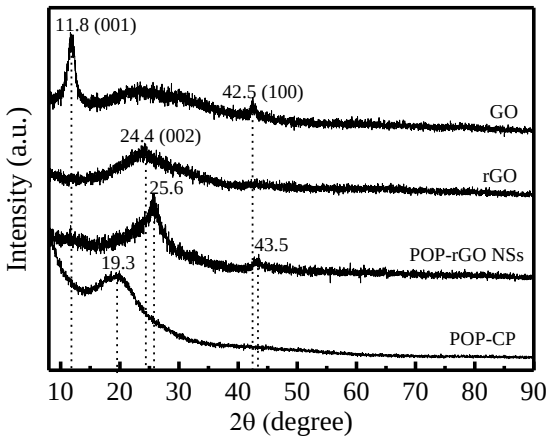

Figure S4. XRD patterns of the prepared samples.

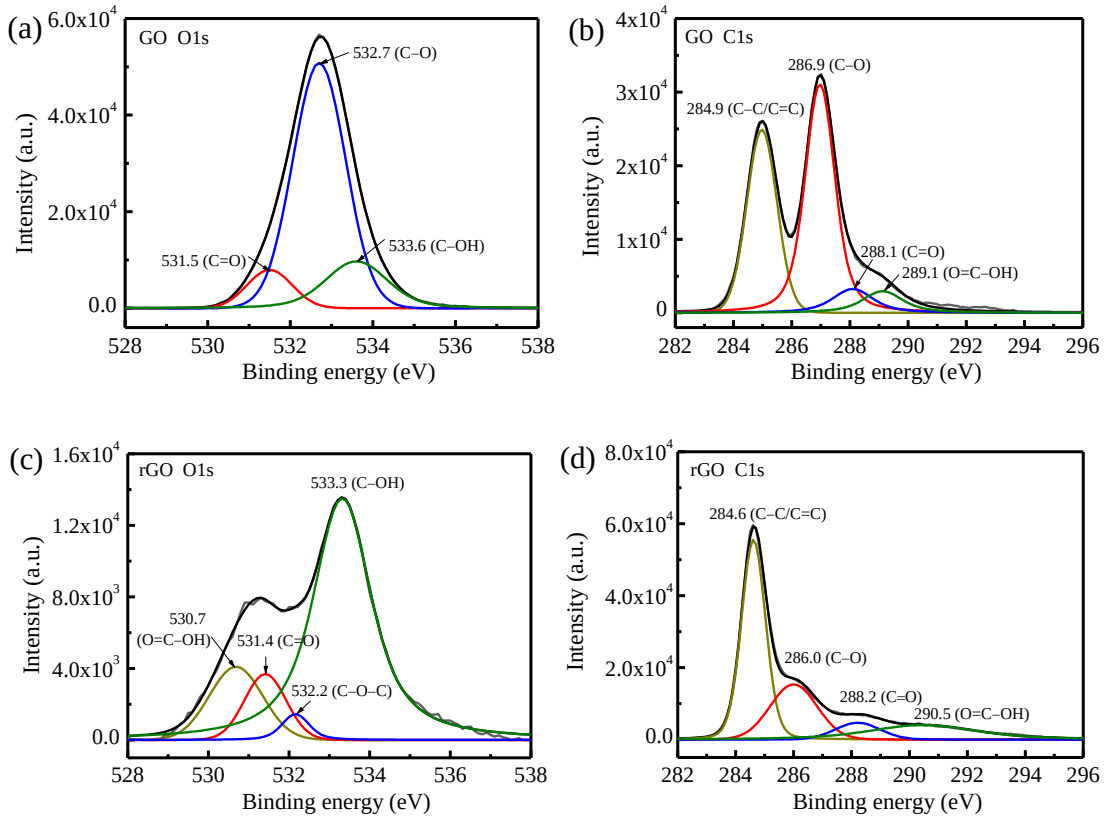

Figure S5. XPS spectra in (a) O1s and (b) C1s of GO; in (c) O1s and (d) C1s of rGO.

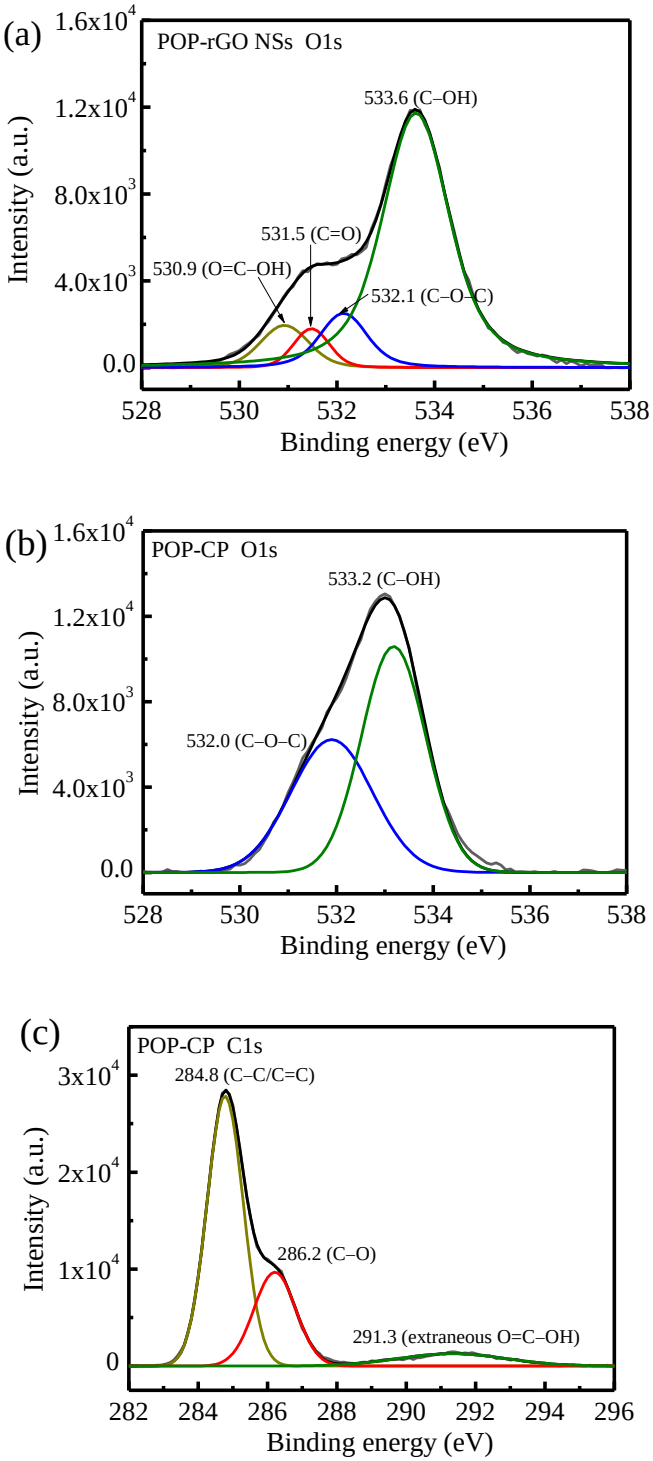

Figure S6. (a) O1s XPS spectra of POP-rGO NSs. (b) O1s and (c) C1s XPS spectra of condensation polymer of POP (POP-CP).

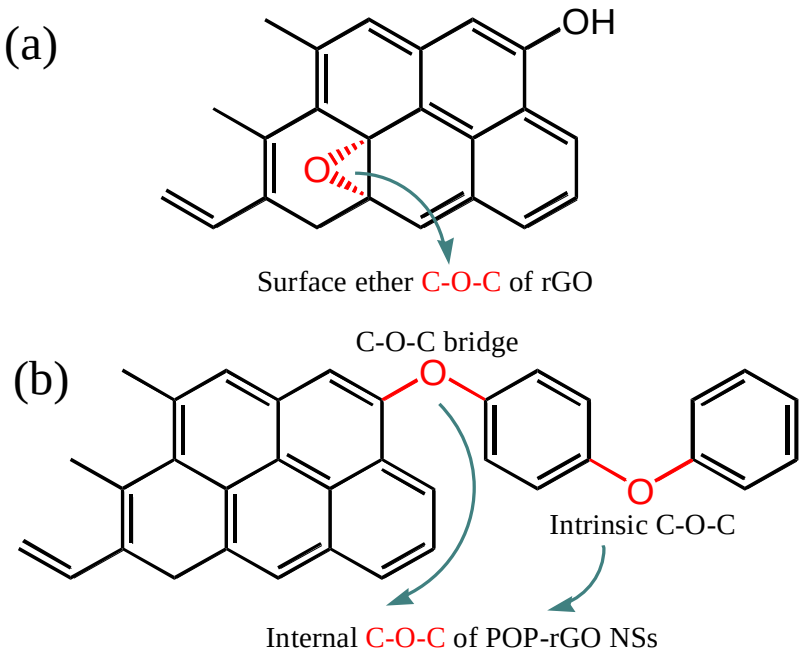

Figure S7. Schematic structure of C-O-C of (a) rGO and (b) POP-rGO NSs.

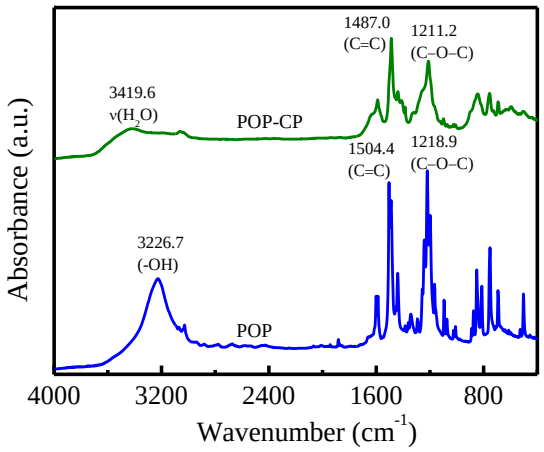

Figure S8. FTIR spectra of POP and the condensation polymer of POP (POP-CP).

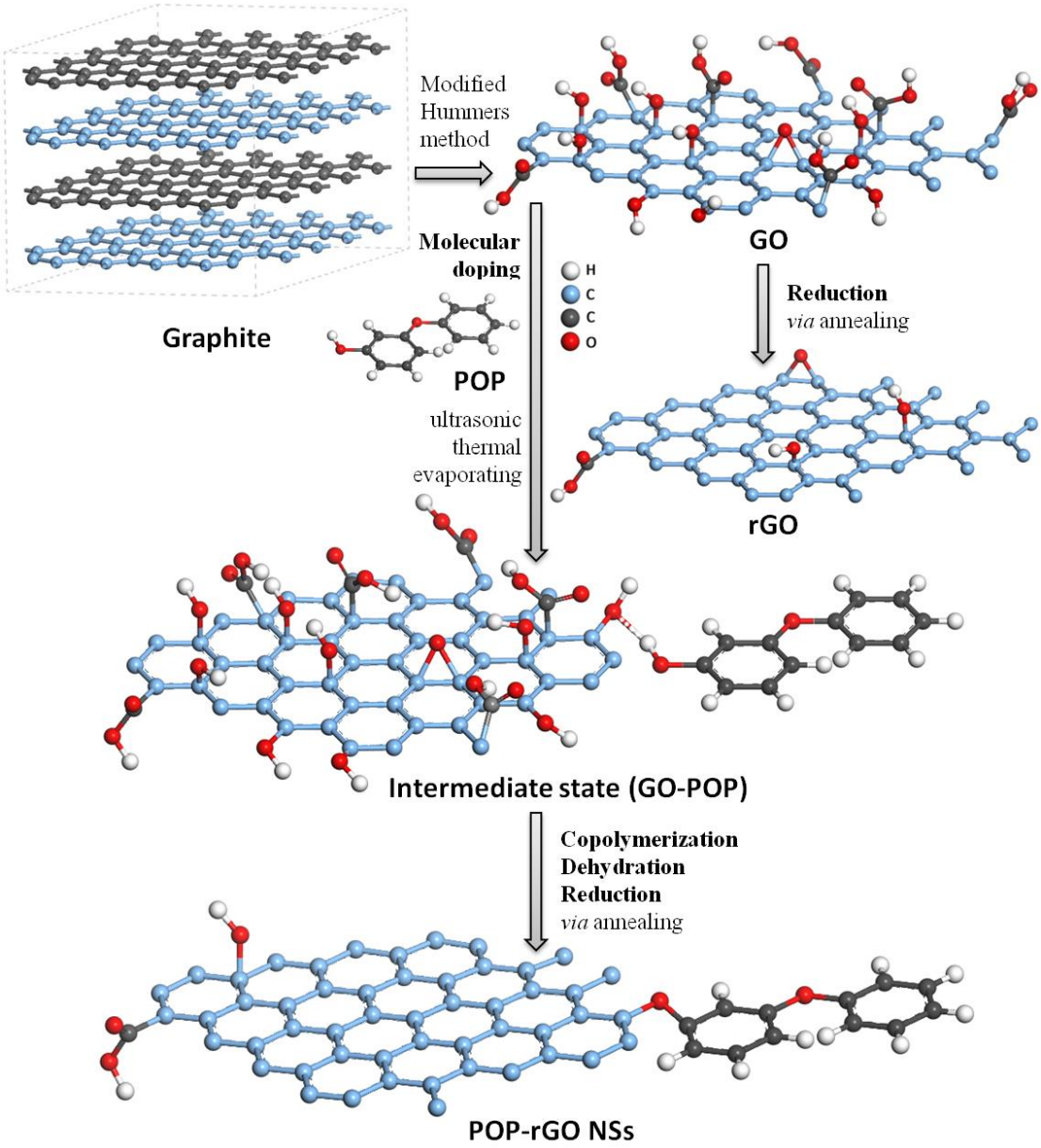

Figure S9. Illustrations for synthesis routes of GO, rGO and POP-rGO NSs and their model structures (The graphene substrate is an infinitely extended structure. The connection between graphene and POP in the illustration does not represent the edge modification).

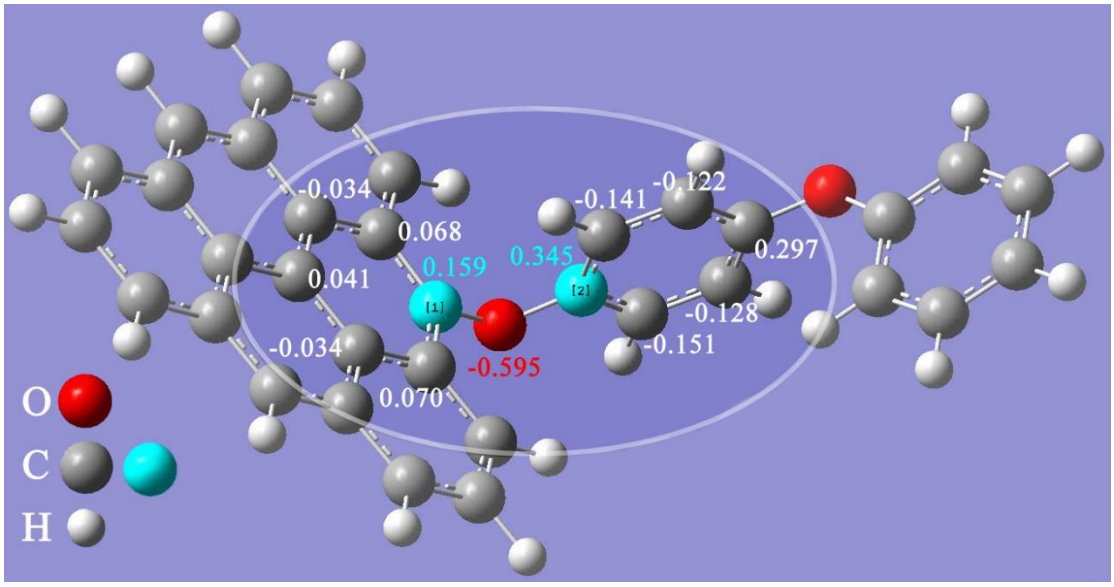

Figure S10. Electric charges for the O and C atoms of POP-rGO NSs *via* DFT calculations.

Table S1. HOMO, LUMO, and HOMO–LUMO energy gap of α electrons and β electrons for POP molecule, graphene (with -OH) and POP-rGO NSs (Unit/eV) [a]

Model fragment	POP molecule		Graphene (-OH)		POP-rGO NSs	
Electrons	α	β	α	β	α	β
HOMO	–5.90	–5.90	–4.08	–6.09	–4.90	–5.95
LUMO	–0.30	–0.30	–0.21	–2.21	–1.36	–2.73
HOMO–LUMO gap	5.60	5.60	3.87	3.88	3.54	3.22

[a] HOMO–LUMO gap is the difference between LUMO and HOMO energy levels.

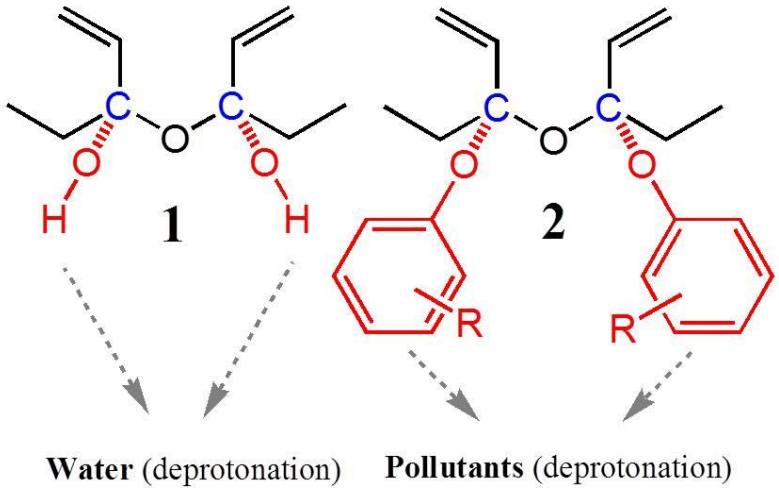

Figure S11. The complexation forms of the electron-poor site C in C-O-C of POP-rGO NSs with water and pollutants.

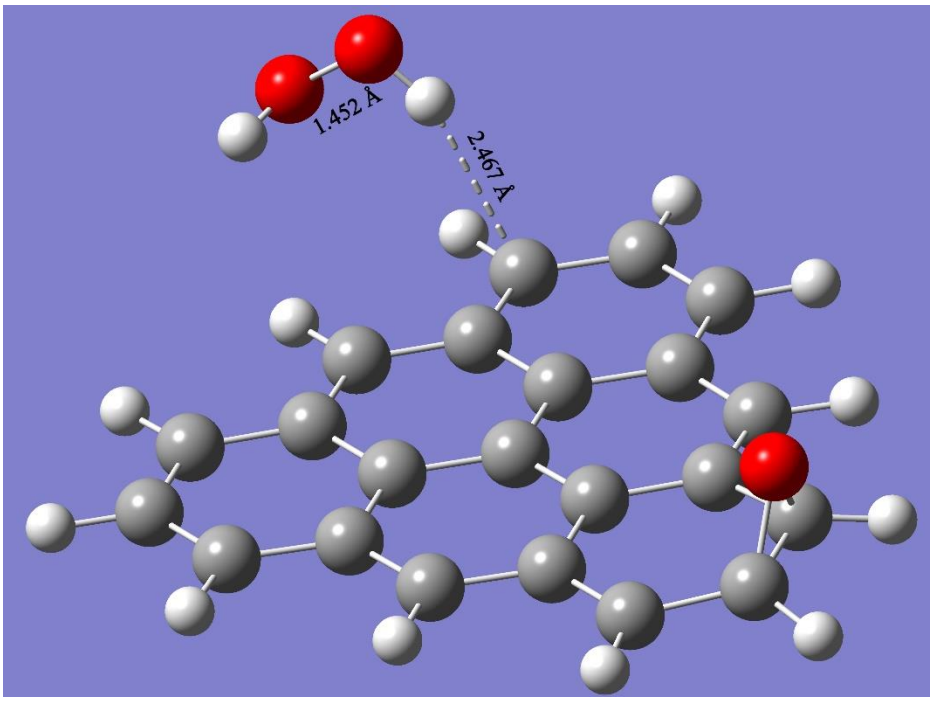

Figure S12. The obtained H_2O_2 absorbing models on the graphene (with surface ether C-O-C) through DFT calculation.

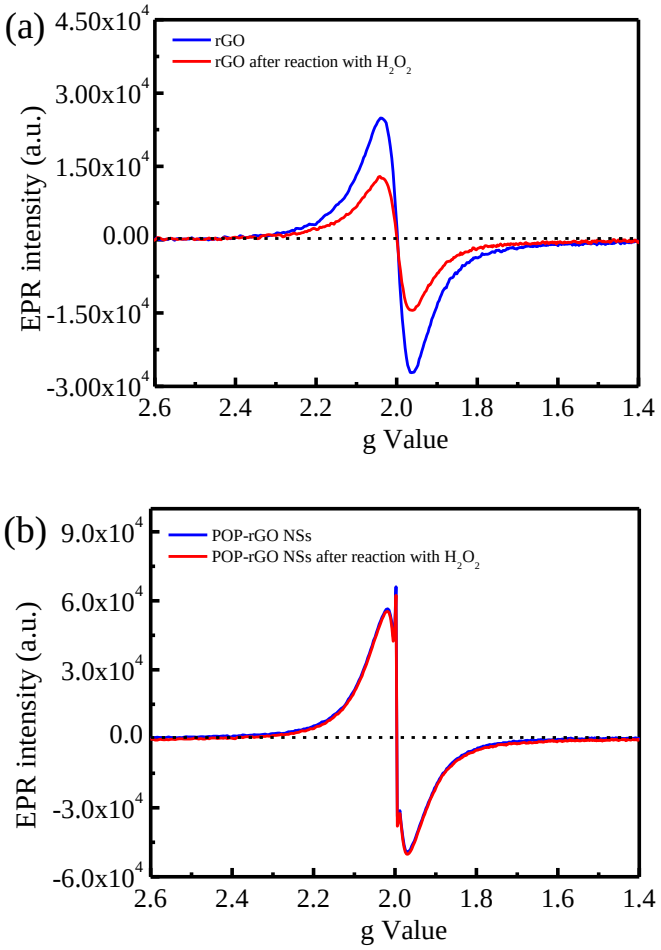

Figure S13. EPR spectra of the (a) rGO and (b) POP-rGO NSs solid samples before and after reaction with H_2O_2.

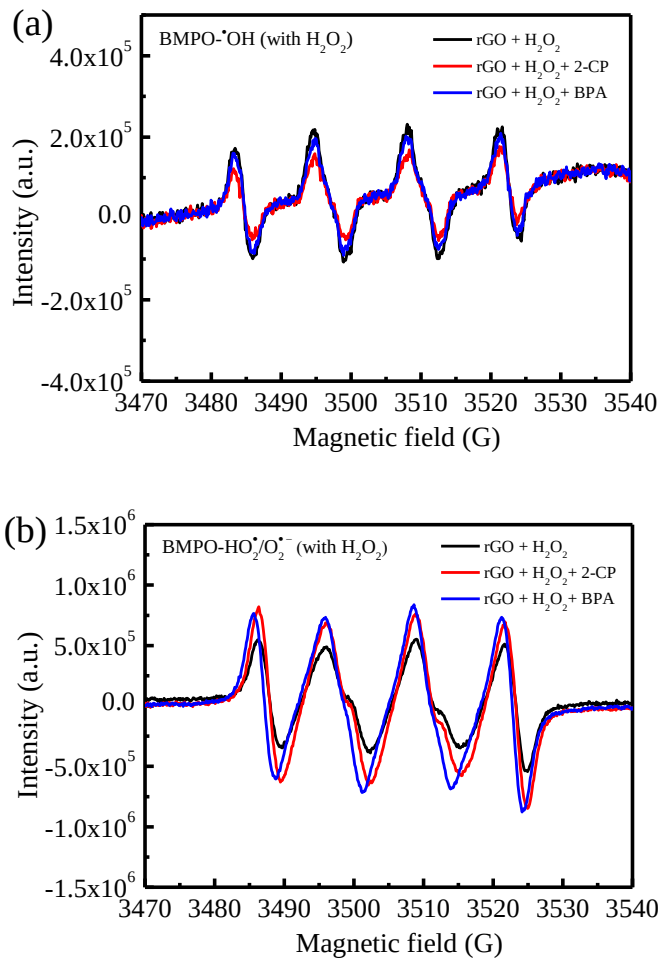

Figure S14. BMPO spin-trapping EPR spectra for (a) $^{\bullet}OH$ in the rGO aqueous suspensions with H_2O_2 and pollutants, and (b) $HO_2^{\bullet}/O_2^{\bullet-}$ in the rGO methanol dispersions with H_2O_2 and pollutants.

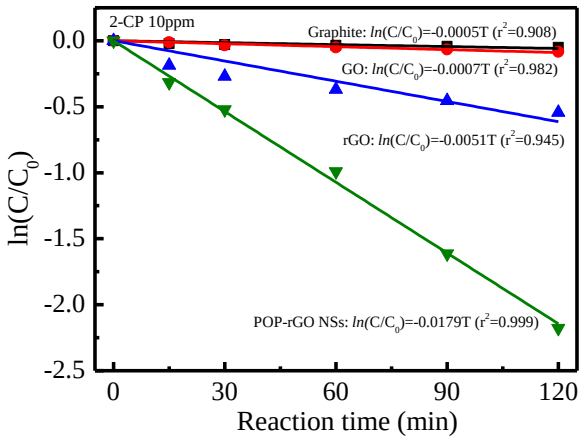

Figure S15. The kinetic curves of 2-CP degradation in various suspensions. Reaction conditions: initial pH 6.5, initial 2-CP 10 ppm, initial H_2O_2 10 mM, catalyst 0.4 g L^{-1}.

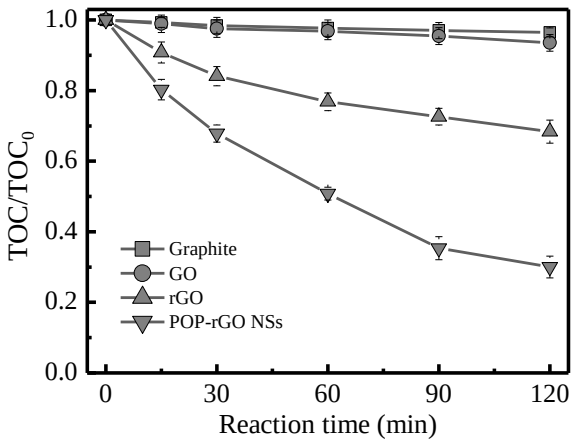

Figure S16. TOC removal curves during 2-CP degradation. Reaction conditions: initial pH 6.5 (nature pH), 2-CP 10 ppm, initial H_2O_2 10 mM, catalyst 0.4 g L^{-1}.

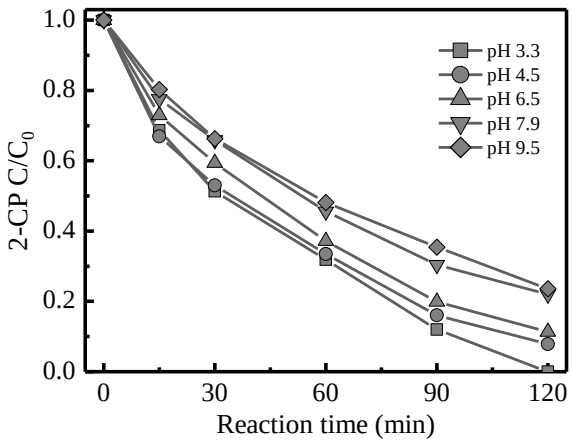

Figure S17. Effect of initial pH values for 2-CP degradation. Reaction conditions: 2-CP 10 ppm, initial H_2O_2 10 mM, catalyst 0.4 g L^{-1}.

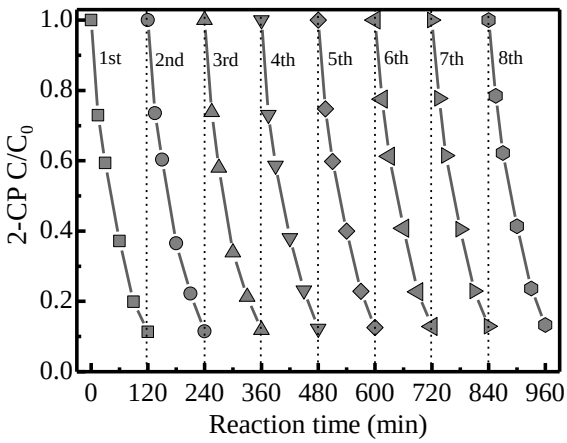

Figure S18. Reusability of POP-rGO NSs for 2-CP degradation. Reaction conditions: initial pH 6.5 (nature pH), 2-CP 10 ppm, initial H_2O_2 10 mM, catalyst 0.4 g L^{-1}.

Supplementary Note:

Calculation of utilization efficiency of H_2O_2. The complete mineralization of one mole 2-CP and BPA will theoretically consume 13 and 36 moles of H_2O_2, respectively (eqs. 1 and 2).

$$C_6H_5OCl+13H_2O_2 \rightarrow 6CO_2+15H_2O+HCl \quad \text{(eq. 1)}$$

$$C_{15}H_{16}O_2+36H_2O_2 \rightarrow 15CO_2+44H_2O \quad \text{(eq. 2)}$$

By measuring the TOC change in the pollutant solutions, the amounts of the mineralized organic pollutants were obtained, and the value of the stoichiometric H_2O_2 consumption ($[\Delta H_2O_2]_S$) for the mineralization of pollutants was calculated on the basis of eq. 1 and 2. The actual H_2O_2 consumption ($[\Delta H_2O_2]_A$) at different reaction time was measured using the DPD method.[3] According to the reported method,[4] The utilization efficiency of H_2O_2 (η) is defined as the ratio of the stoichiometric H_2O_2 consumption ($[\Delta H_2O_2]_S$) for the mineralization of pollutants to the actual H_2O_2 consumption ($[\Delta H_2O_2]_A$) in the Fenton-like reaction and is expressed in eq. 3:

$$\eta = [\Delta H_2O_2]_S / [\Delta H_2O_2]_A \quad \text{(eq. 3)}$$

Supplementary References

1. Hummers, W. S.; Offeman, R. E., Preparation of Graphitic Oxide. *J Am Chem Soc* **1958,** *80*, (6), 1339-1339.

2. Zangmeister, C. D., Preparation and Evaluation of Graphite Oxide Reduced at 220 degrees C. *Chem Mater* **2010,** *22*, (19), 5625-5629.

3. Bader, H.; Sturzenegger, V.; Hoigne, J., Photometric-Method for the Determination of Low Concentrations of Hydrogen-Peroxide by the Peroxidase Catalyzed Oxidation of N,N-Diethyl-P-Phenylenediamine (DPD). *Water Res* **1988,** *22*, (9), 1109-1115.

4. Luo, W.; Zhu, L. H.; Wang, N.; Tang, H. Q.; Cao, M. J.; She, Y. B., Efficient Removal of Organic Pollutants with Magnetic Nanoscaled BiFeO3 as a Reusable Heterogeneous Fenton-Like Catalyst. *Environ Sci Technol* **2010,** *44*, (5), 1786-1791.